

(Cu₂S₂)(Sr₃Sc₂O₅)—A Layered, Direct Band Gap, p-Type Transparent Conducting Oxychalcogenide: A Theoretical Analysis.

David O. Scanlon* and Graeme W. Watson*

School of Chemistry, Trinity College Dublin, Dublin 2, Ireland

Received July 23, 2009. Revised Manuscript Received October 14, 2009

Development of a p-type TCO to rival the high-performance n-type TCOs presently utilized in many applications is one of the grand challenges for materials scientists. However, most of the p-type TCOs fabricated to date have suffered from limited hole mobilities, low conductivities, and indirect band gaps. Recently, [Cu₂S₂][Sr₃Sc₂O₅] has been identified as a possible p-type TCO material, with improved hole mobility. In this article, we study the geometry and electronic structure of [Cu₂S₂][Sr₃Sc₂O₅] using both GGA + *U* and HSE06. We show conclusively that [Cu₂S₂][Sr₃Sc₂O₅] is a direct band gap material, with a hole effective mass at the valence band maximum that indicates the potential for good p-type conductivity, consistent with the reported experimental results. These results are discussed in relation to other p-type TCO materials.

Introduction

Transparent conducting oxides (TCOs) have been studied for more than a hundred years¹ and are important materials in the field of optoelectronics.² These unique materials usually possess carrier concentrations of at least $1 \times 10^{20} \text{ cm}^{-3}$ and optical band gaps greater than 3 eV, and find applications in solar cells, flat panel displays, invisible security circuits etc.³ Although most of the industry standard TCOs are n-type (e.g., SnO₂:F,⁴ In₂O₃:Sn⁵ and ZnO:Al⁶), the development of p-type TCOs has proved very challenging. A p-type TCO with conductivity comparable with the high performance n-type TCOs ($\sim 1 \times 10^4 \text{ S cm}^{-1}$) would open up the possibility of “transparent electronics”.⁷ Thus development of a high figure of merit p-type TCO is a major goal for materials scientists.

The great difficulty with making p-type TCOs stems from the valence band (VB) makeup of most wide band gap binary oxides. These oxides (In₂O₃, ZnO, SnO₂, TiO₂, Ga₂O₃, etc.) possess VBs with O 2p states dominating at the valence band maximum (VBM). In these systems, formation of p-type (acceptor forming) defects is relatively facile, but results in strongly localized, deep lying holes centered on single oxygen sites, which are strongly

coupled to a lattice distortion.⁸ These highly localized holes place a huge limit on any conductivity.⁸ Despite this, doping of these n-type materials to make them p-type has been attempted for decades, and research in this area is still ongoing.^{9,10}

In 1997, a different methodology for designing p-TCOs was proposed by Hosono and co-workers,¹¹ when they reported simultaneous p-type conductivity and optical transparency in thin films of delafossite structured CuAlO₂. Their theory, subsequently called “chemical modulation of the valence band”, postulated that combining the valence band features of Cu₂O (a native p-type oxide with an optical band gap of $\sim 2.17 \text{ eV}$, which precludes it as a TCO¹²) with the larger band gaps of other binary trivalent oxides was an appealing method of developing p-type TCOs.¹³ The occupied Cu 3d states in Cu₂O hybridize with the O 2p states at the top of the VB, with Cu d states dominating at the VBM.¹² Thus, upon hole formation (due to oxygen excess), 3d¹⁰ Cu^I is oxidized to 3d⁹ Cu^{II},¹² creating holes on Cu ions. As the Cu states are hybridized with oxygen, this leads to *less* localized holes with increased mobility. As these valence band features are still inherent in CuAlO₂, CuAlO₂ retains the p-type features of Cu₂O.¹¹

The optical transparency of CuAlO₂ is thought to occur because of the breaking of the dimensionality in the Cu–Cu interactions in CuAlO₂ compared to Cu₂O. In

*To whom correspondence should be addressed. E-mail: scanloda@tcd.ie; watson@g.tcd.ie.

- (1) Ingram, B. J.; Gonzalez, G. B.; Kammler, D. R.; Bertoni, M. I.; Mason, T. O. *J. Electroceram.* **2004**, *13*, 167–175.
- (2) Hayashi, K.; Matsui, S.; Kamiya, T.; Hirano, M.; Hosono, H. *Nature* **2002**, *419*, 462–465.
- (3) Gordon, R. G. *MRS Bull.* **2000**, *25*, 52–57.
- (4) Godinho, K. G.; Walsh, A.; Watson, G. W. *J. Phys. Chem. C* **2008**, *113*, 439–448.
- (5) Walsh, A.; Da Silva, J. L. F.; Wei, S. H.; Korber, C.; Klein, A.; Piper, L. F. J.; DeMasi, A.; Smith, K. E.; Panaccione, G.; Torelli, P.; Payne, D. J.; Bourlange, A.; Egdel, R. G. *Phys. Rev. Lett.* **2008**, *100*, 167402.
- (6) Kohan, A. F.; Ceder, G.; Morgan, D.; Van de Walle, C. G. *Phys. Rev. B* **2000**, *61*, 15019–15027.
- (7) Thomas, G. *Nature* **1997**, *389*, 907.

- (8) Schirmer, O. F. *J. Phys.: Condens. Matter* **2006**, *18*, R667–R704.
- (9) Li, J.; Wei, S. H.; Li, S. S.; Xia, J. B. *Phys. Rev. B* **2006**, *74*, 081201.
- (10) Yan, J. B.; Li, Y. F.; Wei, S. H.; Al-Jassim, M. M. *Phys. Rev. Lett.* **2007**, *98*, 135506.
- (11) Kawazoe, H.; Yasakuwa, H.; Hyodo, H.; Kurita, M.; Yanagi, H.; Hosono, H. *Nature* **1997**, *389*, 939.
- (12) Hu, J. P.; Payne, D. J.; Egdel, R. G.; Glans, P. A.; Learmonth, T.; Smith, K. E.; Guo, J.; Harrison, N. M. *Phys. Rev. B* **2008**, *77*, 155115.
- (13) Kawazoe, H.; Yanagi, H.; Ueda, K.; Hosono, H. *MRS Bull.* **2000**, *25*, 28–36.

Cu₂O, the crystal structure can be thought of as being composed of two interpenetrating cristobalite lattices,^{14,15} with the relatively small band gap thought to be caused by the three-dimensional interactions between the 3d¹⁰ electrons on neighboring Cu^I ions.¹⁶ In the delafossite structure, the dimensionality of the Cu–Cu interactions is decreased, resulting in band gaps large enough for TCO applications.¹⁷

Since Hosono's pioneering study in 1997, an aggressive research drive has been focused on developing other Cu^I based TCOs using the principles of "chemical modulation of the valence band".¹⁸ This has resulted in the identification of other copper Delafossite materials with p-type TCO properties, including CuInO₂,¹⁹ CuScO₂,²⁰ CuCrO₂,²¹ CuGaO₂,²² CuYO₂,²³ and most recently CuBO₂.^{24,25} As these materials are all either limited by an indirect band gap or low conductivity, or both, alternative Cu^I-based materials have been investigated. SrCu₂O₂ was also found to have p-type ability and transparency, even having a direct band gap, but with lower conductivities even than the delafossites.²⁶ To date, the p-type TCO with the highest conductivity is a delafossite (Mg doped CuCrO₂),²¹ which has a conductivity of 220 S cm⁻¹, which is an order of magnitude lower than the n-types.

These band-engineering concepts are not solely centered on materials with oxygen as the anion, and can also be applied to chalcogenides such as sulphides and selenides.²⁷ Chalcogenides, however, suffer from much narrower band-gaps than oxides,²⁸ but have greater hole mobility due to stronger hybridization of the chalcogens with the Cu 3d states at the VBM. Layered oxychalcogenides on the other hand, can maintain the wide band-gaps of the oxides, allied with the increased hybridization of the chalcogen, Ch p⁶ (Ch = S, Se, Te) and Cu 3d¹⁰ states at the VBM. These materials have common [Cu₂Ch₂]²⁻ layers between oxide layers with ionic cations (e.g., La, Sr etc.), with the Cu–Ch bonds forming VBMs

with increased hybridization relative to the Cu–O VBMs in Cu^I-based TCOs.²⁹

LaCuOS was first identified by Hosono and co-workers as a p-type TCO in 2000.³⁰ This layered oxysulfide possessed a band gap of 3.1 eV and when Sr doped showed p-type conductivity of 2.6×10^{-1} S cm⁻¹.³¹ Replacing the chalcogen in the structure with Se results in a p-type material with increased conductivity, but a decreased bandgap.³² In fact, Mg-doped LaCuOSe displayed a very promising conductivity of 910 S cm⁻¹, a hole concentration greater than 1×10^{21} cm⁻³, and hole mobilities as high as 3.5 cm² V⁻¹ s⁻¹.³³ However, the optical band gap of this material is only 2.8 eV, effectively ruling it out as a possible TCO.³³ This illustrates, however, the ability of chalcogen anions, allied with Cu^I cations to be good candidate p-type materials. The challenge remains to engineer a layered oxychalcogenide with sufficient p-type conductivity and better transparency, to equal the performance of the n-type TCOs.

Recently, Liu et al. have synthesized [Cu₂S₂][Sr₃Sc₂O₅] (denoted SCSOS from now on), a very promising layered p-type transparent conducting oxychalcogenide, Figure 1.³⁴ This oxysulfide is composed of layers of [Cu₂S₂]²⁻, as seen in LaCuOS and BaCu₂S₂, but sandwiched between perovskite like [Sr₃Sc₂O₅]²⁺ layers.³⁴ The highly ionic components of the perovskite like layer are thought to be responsible for the optical band gap of 3.1 eV. The p-type conductivity of the undoped material was measured at 2.8 S cm⁻¹, which is higher than the highest undoped conductivity of all the delafossite system (CuBO₂, 1.65 S cm⁻¹),²⁴ and is 2 orders of magnitude higher than the undoped conductivity of LaCuOS (0.01–0.1 S cm⁻¹).³⁴ This relatively high undoped conductivity relative to other Cu^I materials is quite remarkable as the carrier concentration in undoped SCSOS is relatively low at 1×10^{17} cm⁻³.³⁴ One explanation for this is the extremely high hole mobility of SCSOS, which at 150 cm² V⁻¹ s⁻¹ at room temperature, is the highest hole mobility of any p-type TCO, and also is higher than the highest mobility reported for n-type TCOs (In₂O₃: Mo, 130 cm² V⁻¹ s⁻¹).³⁴

In this study we use density functional theory (GGA+U and HSE06) to investigate the geometry and electronic structure of SCSOS. We show conclusively that (i) The VB features of SCSOS are consistent with other Cu^I based layered oxysulfides, (ii) the dispersion and effective hole masses at the VBM are consistent with the high reported conductivity of SCSOS, and (iii) that the minimum optical band gap is direct, making it potentially

- (14) Önsten, A.; Månsson, M.; Claesson, T.; Muro, T.; Matsushita, T.; Nakamura, T.; Kinoshita, T.; Karlsson, U. O.; Tjernberg, O. *Phys. Rev. B* **2007**, *76*, 115127.
- (15) Laskowski, R.; Blaha, P.; Schwarz, K. *Phys. Rev. B* **2003**, *67*, 075102.
- (16) Yanagi, H.; Inoue, S.; Ueda, K.; Kawazoe, H.; Hosono, H.; Hamada, N. *J. Appl. Phys.* **2000**, *88*, 4059–4163.
- (17) Filippetti, A.; Fiorentini, V. *Phys. Rev. B* **2005**, *72*, 035128.
- (18) Marquardt, M. A.; Ashmore, N. A.; Cann, D. P. *Thin Solid Films* **2006**, *496*, 146–156.
- (19) Yanagi, H.; Hase, T.; Ibuki, S.; Ueda, K.; Hosono, H. *Appl. Phys. Lett.* **2001**, *78*, 1583–1585.
- (20) Duan, N.; Sleight, A. W.; Jayaraj, M. K.; Tate, J. *Appl. Phys. Lett.* **2000**, *77*, 1325.
- (21) Nagarajan, R.; Draeseke, A. D.; Sleight, A. W.; Tate, J. *J. Appl. Phys.* **2001**, *89*, 8022.
- (22) Ueda, K.; Hase, T.; Yanagi, H.; Kawazoe, H.; Hosono, H.; Ohta, H.; Orita, M.; Hirano, M. *J. Appl. Phys.* **2001**, *89*, 1790–1793.
- (23) Nagarajan, R.; Duan, N.; Jayaraj, M. K.; Li, J.; Vanaja, K. A.; Yokochi, A.; Draeseke, A.; Tate, J.; Sleight, A. W. *Intl. J. Inorg. Mater.* **2001**, *3*, 265–270.
- (24) Snure, M.; Tiwari, A. *Appl. Phys. Lett.* **2007**, *91*, 092123.
- (25) Scanlon, D. O.; Walsh, A.; Watson, G. W. *Chem. Mater.* **2009**, *21*, 4568–4576.
- (26) Kudo, A.; Yanagi, H.; Hosono, H.; Kawazoe, H. *Appl. Phys. Lett.* **1998**, *73*, 220–222.
- (27) Ueda, K.; Hiramatsu, H.; Hirano, M.; Kamiya, T.; Hosono, H. *Thin Solid Films* **2006**, *496*, 8–15.
- (28) Liu, M. L.; Wu, L. B.; Huang, F. Q.; Chen, L. D.; Ibers, J. A. *J. Solid. State. Chem.* **2007**, *180*, 62–69.

- (29) Clarke, S. J.; Adamson, P.; Herkelrath, S. J. C.; Rutt, O. J.; Parker, D. R.; Pitcher, M. J.; Smura, C. F. *Inorg. Chem.* **2008**, *47*, 8473–8486.
- (30) Ueda, K.; Inoue, S.; Hirose, S.; Kawazoe, H.; Hosono, H. *Appl. Phys. Lett.* **2000**, *77*, 2701–2703.
- (31) Jiramatsu, H.; Ueda, K.; Ohta, H.; Orita, M.; Hirano, M.; Hosono, H. *Thin Solid Films* **2002**, *411*, 125–128.
- (32) Ueda, K.; Hosono, H.; Hamada, N. *J. Phys. Condens. Matter* **2004**, *16*, 5179–5186.
- (33) Hiramatsu, H.; Ueda, K.; Ohta, H.; Hirano, H.; Kikuchi, M.; Yanagi, H.; Kamiya, T.; Hosono, H. *Appl. Phys. Lett.* **2007**, *91*, 012104.
- (34) Liu, M. L.; Wu, L. B.; Huang, F. Q.; Chen, L. D.; Chen, I. W. *J. Appl. Phys.* **2007**, *102*, 116108.

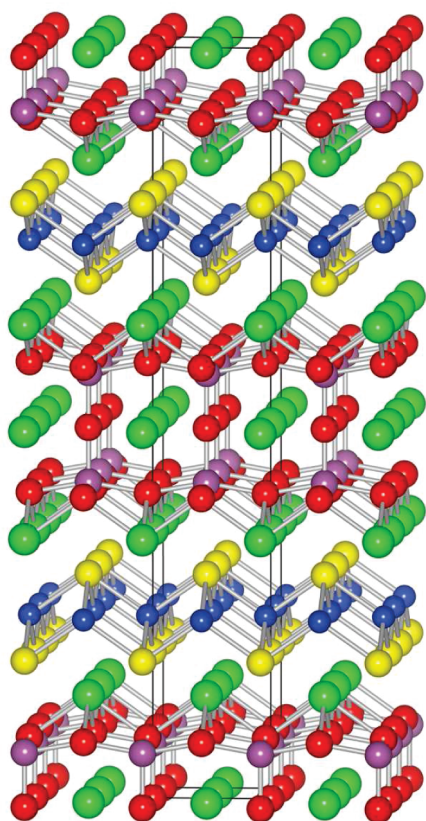


Figure 1. Layered structure of $[\text{Cu}_2\text{S}_2][\text{Sr}_3\text{Sc}_2\text{O}_5]$. The red, blue, yellow, purple, and green balls are oxygen, copper, sulfur, scandium, and strontium, respectively. The unit cell is indicated by the black box.

more useful in optoelectronic devices than indirect band gap materials. The enhanced conductivity and hole mobility of SCSOS compared to other Cu^{I} based materials are discussed and strategies to improve this conductivity are formulated.

Calculation Methodology

All calculations were performed using the periodic DFT code VASP,^{35,36} in which a plane-wave basis set describes the valence electronic states. The Perdew-Burke-Ernzerhof³⁷ (PBE) gradient corrected functional was used to treat the exchange and correlation. The projector-augmented wave^{38,39} (PAW) method was used to describe the interactions between the cores ($\text{Cu}:[\text{Ar}]$, $\text{Sc}:[\text{Ne}]$, $\text{Sr}:[\text{Ar}]$, $\text{S}:[\text{Ne}]$, and $\text{O}:[\text{He}]$) and the valence electrons.

To counteract the errors associated with the DFT self-interaction,⁴⁰ calculations were performed using DFT corrected for on-site Coulombic interactions $\text{GGA}+U$ ⁴¹ and a hybrid density functional (HSE06).⁴² The validity of the $\text{GGA}+U$ approach has been demonstrated in its recent use to provide improved descriptions of a wide range of localized electronic defect

systems including n-type^{43–47} and p-type polarons.^{48,49} The value of U (applied to the Cu d states) used in this study was 5.2 eV, which has recently been shown to reproduce the valence band features of CuAlO_2 ⁵⁰ and CuCrO_2 ⁵¹ from comparison with high-resolution XPS spectra.

Although $\text{GGA}+U$ does provide a definite improvement over generalized gradient approximation/local density approximation (GGA/LDA) descriptions of strongly correlated or polaronic systems, band gaps are still underestimated. Using larger values of U can provide better descriptions of band gaps, but often this is achieved with the unwanted side effects of poor crystal properties of pure or defective systems relative to experiment.⁵² Another approach to counteract the SIE is to utilize hybrid functionals, which include a certain percentage of exact Fock exchange with the DFT exchange and correlation. Unfortunately, hybrid functionals are computationally very demanding, and have in some cases been overlooked in favor of less computationally expensive methods, such as the “ $+U$ ” correction, or even a range of a posteriori corrections to LDA/GGA calculations.⁵³ Hybrid functionals often give better approximations of band gaps in semiconductor systems, and provide improved structural data.⁵⁴ In this study, we have used the screened hybrid density functional developed by Heyd, Scuseria and Ernzerhof (HSE06),⁴² as implemented in the VASP code.⁵⁵ Difficulties in evaluating the Fock exchange in a real space formalism are caused by the slow decay of the exchange interaction with distance. In the HSE06 hybrid functional approach, this problem is addressed by separating the description of the exchange interaction into long and a short-range parts,⁴² with a percentage ($\alpha = 25\%$) of exact nonlocal Fock exchange replacing the short-range (SR) PBE functional. A screening of $\omega = 0.11 \text{ bohr}^{-1}$ is applied to partition the Coulomb potential into long-range (LR) and SR terms, which gives:

$$E_{xc}^{\text{HSE06}}(\omega) = E_x^{\text{HSE06, SR}} + E_x^{\text{PBE, LR}} + E_c^{\text{PBE}} \quad (1)$$

where

$$E_x^{\text{HSE06, SR}} = \frac{1}{4} E_x^{\text{Fock, SR}} + \frac{3}{4} E_x^{\text{PBE, SR}} \quad (2)$$

Fock and PBE exchange are therefore only mixed in the SR part, with the LR exchange interactions being represented by the corresponding part of the range separated PBE functional.⁴² The HSE06 functional has been shown to produce structural

- (35) Kresse, G.; Furthmüller, J. *Phys. Rev. B* **1996**, *54*, 11169–11186.
- (36) Kresse, G.; Hafner, J. *Phys. Rev. B* **1994**, *49*, 14251–14271.
- (37) Perdew, J. P.; Burke, K.; Ernzerhof, M. *Phys. Rev. Lett.* **1996**, *77*, 3865.
- (38) Blöchl, P. E. *Phys. Rev. B* **1994**, *50*, 17953.
- (39) Kresse, G.; Joubert, D. *Phys. Rev. B* **1999**, *59*, 1758–1775.
- (40) Morgan, B. J.; Scanlon, D. O.; Watson, G. W. *J. Surf. Sci. Nanotechnol.* **2009**, *7*, 395–404.
- (41) Dudarev, S. L.; Botton, G. A.; Savrasov, S. Y.; Humphreys, C. J.; Sutton, A. P. *Phys. Rev. B* **1998**, *57*, 1505.
- (42) Heyd, S.; Scuseria, G. E.; Ernzerhof, M. *J. Chem. Phys.* **2003**, *118*, 8207–8215.

- (43) Morgan, B. J.; Watson, G. W. *Surf. Sci.* **2007**, *601*, 5034–5041.
- (44) Scanlon, D. O.; Walsh, A.; Morgan, B. J.; Watson, G. W. *J. Phys. Chem. C* **2008**, *112*, 9903–9911.
- (45) Coquet, R.; Willock, D. J. *Phys. Chem. Chem. Phys.* **2005**, *7*, 3819–3828.
- (46) Walsh, A.; Yan, Y.; Al-Jassim, M. M.; Wei, S. H. *J. Phys. Chem. C* **2008**, *112*, 12044–12050.
- (47) Morgan, B. J.; Scanlon, D. O.; Watson, G. W. *J. Mater. Chem.* **2009**, *19*, 5175–5178.
- (48) Nolan, M.; Watson, G. W. *J. Chem. Phys.* **2006**, *125*, 144701–6.
- (49) Scanlon, D. O.; Walsh, A.; Morgan, B. J.; Nolan, M.; Fearon, J.; Watson, G. W. *J. Phys. Chem. C* **2007**, *111*, 7971–7979.
- (50) Scanlon, D. O.; Walsh, A.; Morgan, B. J.; Watson, G. W.; Payne, D. J.; Egdel, R. G. *Phys. Rev. B* **2009**, *79*, 035101.
- (51) Arnold, T.; et al. *Phys. Rev. B* **2009**, *79*, 075102.
- (52) Laubach, S.; Schmidt, P. C.; Thissen, A.; Fernandez-Madrigal, F. J.; Wu, Q. H.; Jaegermann, W.; Klemm, M.; Horn, S. *Phys. Chem. Chem. Phys.* **2007**, *9*, 2564–2576.
- (53) Raebiger, H.; Lany, S.; Zunger, A. *Phys. Rev. B* **2007**, *76*, 045209.
- (54) Labat, F.; Baranek, P.; Domain, C.; Minot, C.; Adamo, C. *J. Chem. Phys.* **2007**, *126*, 154703.
- (55) Paier, J.; Marsman, M.; Hummer, K.; Kresse, G.; Gerber, I. C.; Ángyán, J. G. *J. Chem. Phys.* **2006**, *124*, 154709–154713.

and band gap data that are more accurate than LDA/GGA and meta-GGA data.^{56–60}

Structural optimizations of bulk SCSOS were performed using GGA+*U* and HSE06 at a series of volumes in order to calculate the equilibrium lattice parameters. In each case, the atomic positions, lattice vector and cell angle were allowed to relax, while the total volume was held constant. The resulting energy volume curves were fitted to the Murnaghan equation of state to obtain the equilibrium bulk cell volume.⁶¹ This approach minimizes the problems of Pulay stress and changes in basis set which can accompany volume changes in plane wave calculations. The Pulay stress affects the stress tensor that is not used in obtaining the optimized lattice vectors and hence this approach is significantly more accurate than using the stress tensor to perform constant pressure optimization. Convergence with respect to *k*-point sampling and plane wave energy cut off were checked, and for GGA+*U* a cutoff of 500 eV and for HSE06 a cutoff of 400 eV were found to be sufficient. In both cases a *k*-point sampling of $6 \times 6 \times 1$ were found to be sufficient. Calculations were deemed to be converged when the forces on all the atoms were less than $0.01 \text{ eV } \text{\AA}^{-1}$.

The optical transition matrix elements and the optical absorption spectrum were calculated within the transversal approximation and PAW method.⁶² Within this methodology, the adsorption spectra is summed over all direct VB to CB transitions and therefore ignores indirect and intraband absorptions.⁶³ In this framework of single-particle transitions, the electron–hole correlations are not treated, and thus would need treatment by higher-order electronic structure methods.^{64,65} This method, however, has been previously shown to provide reasonable optical absorption spectra.^{59,66,67} Structure and charge density visualization and analysis were performed using VESTA.⁶⁸

Results

SCSOS crystallizes in the *I4/mmm* space group, with anti-PbO (litharge⁶⁹) structured layers of $[\text{Cu}_2\text{S}_2]^{2-}$ alternating with perovskite like layers of $[\text{Sr}_3\text{Sc}_2\text{O}_5]^{2+}$, Figure 1.³⁴ The GGA + *U* and HSE06 calculated lattice parameters and interatomic bond distances for SCSOS are shown in Table 1. The GGA + *U* results slightly overestimate the lattice constants, as is to be expected from a GGA calculation,⁵⁰ but are within by 0.7% of the experimental values. The HSE06 calculations produced

Table 1. Structural Data and Nearest-Neighbour Interatomic Distances for the GGA + *U* and HSE06 Optimized $[\text{Cu}_2\text{S}_2][\text{Sr}_3\text{Sc}_2\text{O}_5]$ and the Experimental Data from the Work of Otzsch et al.;⁷⁵ Volumes are Given in \AA^3 and Lattice Dimensions and Interatomic Distances in \AA

	GGA + <i>U</i>	HSE06	experiment ⁷⁵
<i>V</i>	440.86	424.05	431.67
<i>a</i>	4.10	4.06	4.08
<i>c</i>	26.18	25.74	25.99
Cu–S	2.443	2.429	2.489
	2.554	2.520	2.515
Sr–O	2.901	2.870	2.882
	3.058	3.012	3.046
Sc–O	2.069	2.045	2.070
	1.997	1.972	1.903
Cu–Cu	2.901	2.873	2.882

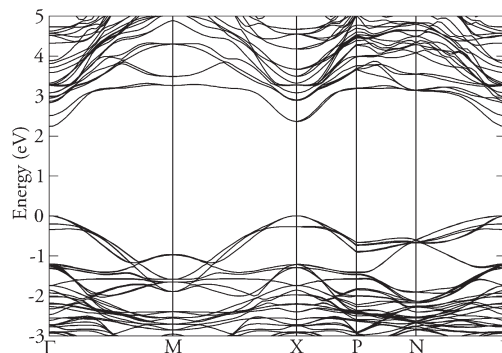


Figure 2. GGA + *U* calculated band structure of $[\text{Cu}_2\text{S}_2][\text{Sr}_3\text{Sc}_2\text{O}_5]$. The top of the valence band is set to 0 eV.

lattice constants slightly underestimated compared to the experimental data. Interestingly the Cu–Cu distances in SCSOS are 2.882 \AA , which are longer than the Cu–Cu distances in LaCuOSe (2.876 \AA) and virtually equivalent to the Cu–Cu distances in LaCuOS (2.8826 \AA).⁷⁰ This result is quite surprising, as the Cu–Cu distances in copper delafossites can be a limiting factor in p-type conduction, as delafossites are governed by a polaronic hole hopping conduction mechanism.^{71–74} In delafossite materials, the hole hops from Cu to Cu, making a shorter Cu–Cu distance extremely beneficial for good undoped conductivity.⁷¹ The conductivity of undoped SCSOS is known to be higher than that of LaCuOS and LaCuOSe,³⁴ so it would appear that the Cu–Cu distances do not have as significant an effect on conductivities in these layered oxychalcogenides.

The GGA + *U* calculated band structure of SCSOS along the high symmetry lines taken from Bradley and Cracknell⁷⁶ is shown in Figure 2. Both the VBM and the conduction band minimum (CBM) are situated at the

- (56) Heyd, J.; Scuseria, G. E. *J. Chem. Phys.* **2004**, *121*, 1187–1192.
 (57) Heyd, J.; Peralta, J. E.; Scuseria, G. E.; Martin, R. L. *J. Chem. Phys.* **2005**, *123*, 174101.
 (58) Da Silva, J. L. F.; Ganduglia-Pirovano, M. V.; Sauer, J.; Bayer, V.; Kresse, G. *Phys. Rev. B* **2007**, *75*, 045121.
 (59) Walsh, A.; Da Silva, J. L. F.; Yan, Y.; Al-Jassim, M. M.; Wei, S. H. *Phys. Rev. B* **2009**, *79*, 073105.
 (60) Chen, S.; Gong, Z. G.; Walsh, A.; Wei, S. H. *Appl. Phys. Lett.* **2009**, *94*, 041903.
 (61) Murnaghan, F. D. *Proc. Natl. Acad. Sci. U.S.A.* **1944**, *30*, 244–247.
 (62) Gajdos, M.; Hummer, K.; Kresse, G.; Furthmüller, J.; Bechstedt, F. *Phys. Rev. B* **2006**, *73*, 045112.
 (63) Adolph, B.; Furthmüller, J.; Bechstedt, F. *Phys. Rev. B* **2001**, *63*, 125108.
 (64) Ramos, L. E.; Paier, J.; Kresse, G.; Bechstedt, F. *Phys. Rev. B* **2008**, *78*, 195423.
 (65) Paier, J.; Marsman, M.; Kresse, G. *Phys. Rev. B* **2008**, *78*, 121201.
 (66) Nie, X.; Wei, S. H.; Zhang, S. B. *Phys. Rev. Lett.* **2002**, *88*, 066405.
 (67) Walsh, A.; Yan, Y.; Huda, M. N.; Al-Jassim, M. M.; Wei, S. H. *Chem. Mater.* **2009**, *21*, 547–551.
 (68) Momma, K.; Izumi, F. *J. Appl. Crystallogr.* **2008**, *41*, 653–658.
 (69) Walsh, A.; Watson, G. W. *J. Solid-State Chem.* **2005**, *178*, 1422–1428.

- (70) Ueda, K.; Hosono, H. *Thin Solid Films* **2002**, *411*, 115–118.
 (71) Benko, F. A.; Koffyberg, F. P. *J. Phys. Chem. Solids* **1987**, *48*, 431–43.
 (72) Ingram, B. J.; Mason, T. O.; Asahi, R.; Park, K. T.; Freeman, A. J. *Phys. Rev. B* **2001**, *64*, 155114.
 (73) Ingram, B. J.; Gonzalez, G. B.; Mason, T. O.; Shahriari, D. Y.; Barnabe, A.; Ko, D.; Poepplmeier, K. R. *Chem. Mater.* **2004**, *16*, 5616–5622.
 (74) Ingram, B. J.; Harder, B. J.; Hrabe, N. W.; Mason, T. A.; Poepplmeier, K. R. *Chem. Mater.* **2004**, *16*, 5623–5629.
 (75) Otzsch, K.; Ogino, H.; Shimoyama, J.; Kishio, K. *J. Low Temp. Phys.* **1999**, *117*, 729–733.
 (76) Bradley, C. J.; Cracknell, A. P. *Mathematical Theory of Symmetry in Solids*; Oxford University Press: Oxford, U.K., 1972.

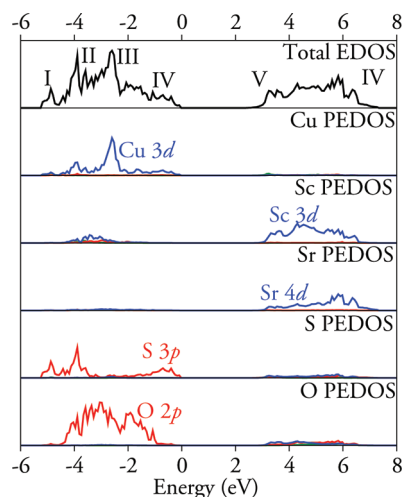


Figure 3. Electronic density of states for $[\text{Cu}_2\text{S}_2][\text{Sr}_3\text{Sc}_2\text{O}_5]$. (a) Total EDOS, (b) Cu PEDOS, (c) Sc PEDOS, (d) Sr PEDOS, (e) S PEDOS, and (f) O PEDOS. The black lines represent total EDOS, blue lines represent d states, green s states, and red p states.

Γ point, indicating that SCSOS is a direct band gap material. LaCuOS and LaCuOSe are also direct band gap materials, although BiCuOS and BiCuOSe are both indirect band gap materials, showing the sensitivity of the electronic structure of these layered materials to the choice of ionic cation in the non- $[\text{Cu}_2\text{S}_2]^{2-}$ layer.⁷⁷ The VBM at Γ displays promising dispersion, especially in the Γ –M direction, which can be viewed as being indicative of good p-type ability. This VB dispersion is visibly larger than that of any of the Cu^{I} based delafossites^{25,50,51} or of SrCu_2O_2 .⁷⁸

The GGA + U direct band gap, measured at the Γ point, is 2.12 eV. This is an underestimation of the experimentally measured optical band gap of 3.1 eV, but is to be expected as GGA + U calculations are known to produce underestimated band gaps.⁵⁰ The HSE06 calculated direct band gap at the Γ point is 3.19 eV, which is in excellent agreement with the experimental value. HSE06 is expected to predict band gaps that are more consistent with experiment than those of LDA/GGA/GGA + U methods.^{56–60}

The calculated total and partial (ion decomposed) electronic densities of states (EDOS/PEDOS) for SCSOS is shown in Figure 3a–f. The PEDOS were calculated by projecting wave functions onto atom centered spherical harmonics, with radii of 1.45 Å for Cu, 1.1 Å for Sr, 1.1 Å for Sc, 1.1 Å for S, and 1.5 Å for O. The correct number of electrons are reproduced by these radii, and their ratios are consistent with the positions of charge density minima observed in valence-charge density plots. For discussion, the VB is split into four regions (labeled I to IV), with the conduction band split into two regions (V and VI).

Region I lies between -6 eV and -4.5 eV and is composed mainly of sulfur 3p states with some minor

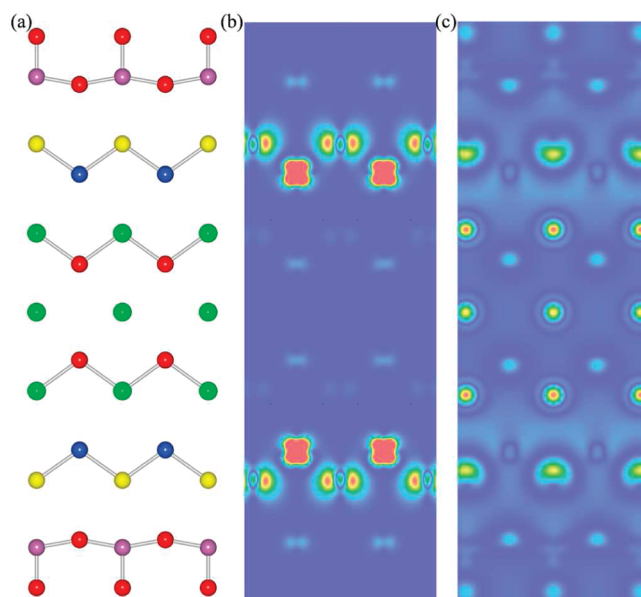


Figure 4. Charge density contour plots showing the band edges of $[\text{Cu}_2\text{S}_2][\text{Sr}_3\text{Sc}_2\text{O}_5]$ through a (010) plane. (a) is the structure of the cell in the (010) plane, (b) is the charge density of the VBM at Γ , and (c) is the charge density of the CBM at Γ , plotted from 0 eV (blue) to 0.003 eV (red) $e \text{ Å}^{-3}$.

mixing of Cu 3d and O 2p. Region II (between -4.5 eV and -3 eV) is dominated by O 2p and S 2p states, with the large peak at -3.8 eV in the EDOS being composed mainly of S 3p, O 2p with some mixing with Cu 3d states, and very minor contributions from Sc 3d states. Between -3 eV and -1 eV (Region III), Cu 3d states dominate with significant mixing with O 2p states and some minor interactions with with Sc 3d and S 3p. Region IV (-1 eV to the VBM), is dominated by hybridized Cu 3d and S 3p states, with very small contribution from O 2p. This is in contrast with the VBM features of most Cu^{I} based delafossites, which have Cu 3d states interacting strongly with O 2p states at the VBM.⁵¹ Similar VBM features to those of SCSOS have been seen for LaCuOCh ($\text{Ch} = \text{S}, \text{Se}, \text{Te}$).³² The bottom of the conduction band (Region V) is dominated by Sr 4d with some mixing with Sc 3d and O and S s states. Region VI (from 4 eV to 8, eV) is predominantly Sr 4d hybridized with Sc 3d states, with some minor mixing with O 2p states.

In an effort to gain insight into the band edge features of SCSOS (the states that will control any conduction), we have plotted the projections of the wave functions for both the VBM and the CBM at the Γ point through a (010) plane containing Cu, S, Sc, Sr and O atoms, labeled (b) and (c) in Figure 4. It is clear from analysis of the VBM, Figure 4 b, that the vast majority of the density resides in the $[\text{Cu}_2\text{S}_2]^{2-}$ layers, with the density on the S ions having p orbital character and the density on the Cu states having d orbital character. A numerical analysis of the states at the VBM shows that it consists of $\sim 49\%$ Sulfur p_x and $\sim 39\%$ copper d_{xy} states. The absence of any significant density on the oxygen ions indicates that oxygen states do not contribute to the p-type conductivity of this layered material.

(77) Hiramatsu, H.; Yanagi, H.; Kamiya, T.; Ueda, K.; Hirano, M.; Hosono, H. *Chem. Mater.* **2008**, *20*, 326–334.

(78) Godinho, K. G.; Watson, G. W.; Walsh, A.; Green, A. J. H.; Payne, D. J.; Harmer, J.; Egdel, R. G. *J. Mater. Chem.* **2008**, *18*, 2798–2806.

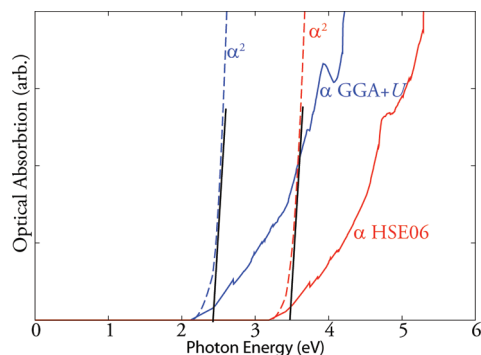


Figure 5. Calculated optical absorption spectrum of $[\text{Cu}_2\text{S}_2][\text{Sr}_3\text{Sc}_2\text{O}_5]$ summed over all possible direct valence to conduction band transitions. GGA + U (blue) and HSE06 (red).

A similar numerical breakdown of the states at the CBM at Γ reveals that it is composed of $\sim 43\%$ sulfur s and p_z states, with $\sim 39\%$ Sr s states and $\sim 12\%$ O p_x states. This is further evidenced by the charge density plot of the CBM, Figure 4c, which clearly shows the polarized s and p_z states on the sulfur, and the s states of Sr and O are visible, with a distinct absence of density on the Sc and Cu states.

The optical absorption spectra for SCSOS, calculated using GGA+ U and HSE06, is shown in Figure 5. For SCSOS we find that fundamental band-edge transitions at the Γ point are symmetry allowed, with absorption beginning at 2.12 eV for GGA+ U and 3.19 eV for HSE06. Using the Tauc relation ($E_g \propto \alpha^2$), we predict the optical band gaps of SCSOS to be 2.41 eV and 3.48 eV using GGA+ U and HSE06 respectively. The HSE06 calculated absorption spectra are in good agreement with the absorption spectra reported from experiment.³⁴

This direct allowed VBM to CBM absorption is in contrast with the absorption behavior of Cu^{I} delafossite TCOs⁶⁶ and the industry standard n-type TCOs In_2O_3 ,⁵ in which transitions from Γ to Γ are symmetry disallowed. Often LDA/GGA U , hybrid functionals or a posteriori corrections⁷⁹ are used to correct band gap problems in theoretical studies of these technologically relevant materials by fitting to the optical band gaps. This “band gap fitting” does not take into account that the magnitude of the direct band gap in these materials is often not the same thing as the optical band gap⁵ and can lead to incorrect positioning of defect levels relative to the band edges.⁸⁰ However, in the case of SCSOS, the direct band gap taken from the band structure does correspond to the optical absorption. A closer analysis of the calculated absorption spectra, Figure 5, shows a gradual ascension to shorter photon wavelengths due to the dispersion at Γ . This is again at variance with the optical absorption spectra for Cu^{I} based delafossites, which display abrupt absorption edges.⁶⁶

Although a large optical band gap is vital for a material to be transparent, p -TCO materials should also have no

Table 2. Effective Hole Masses of $[\text{Cu}_2\text{S}_2][\text{Sr}_3\text{Sc}_2\text{O}_5]$ Calculated Using GGA+ U ; All Hole Effective Masses Given in m_e

	[001]	[010]	[100]	Γ –M
effective hole mass	∞	2.86	2.86	0.96

visible light absorption between the VBM and the bands below.⁸¹ Similarly for n-type TCOs, there should be no absorption between the CBM and the conduction bands above.⁸² For p-type (n-type) TCOs, it is necessary to avoid transitions between unoccupied (occupied) defect bands and the bands within 3.1 eV of the VBM (CBM), meaning that the defective systems are still transparent to visible light.⁸² We have tested the VB-VBM transitions in SCSOS by calculating the dipole transition matrix elements between the VBM and the other VB states at Γ . This analysis revealed that the dipole transition probabilities are negligible between the VBM and states within 3.3 eV below the VBM. This is to be expected, as on-site transitions between states of the same angular momentum (e.g., O p to O p and Cu d to Cu d) are forbidden because of the classical selection rule.⁸¹ The experimental samples of SCSOS examined by Liu et al. were known to contain intrinsic defects,³⁴ yet still report a band gap of 3.1 eV. If transitions between the unoccupied hole states and occupied valence bands within 3.1 eV of the VBM were allowed, the material would not be transparent. Therefore, we conclude that SCSOS has all the attributes of transparency, namely a wide fundamental band gap and no visible light absorption between the VBM and the valence bands below.

The hole effective mass at the VBM of SCSOS has been investigated to gain insights into the materials p -type ability. The effective mass is calculated using:

$$\frac{1}{m^*(E)} = \frac{1}{\hbar^2 k} \frac{dE}{dk} \quad (3)$$

where $E(k)$ is the band edge energy as a function of wave vector k , obtained directly from the GGA + U calculation.⁸³ In this methodology, the diagonal elements of the effective mass tensor can be calculated for a certain k -point. The bands at the top of the VBM are clearly not strictly parabolic in nature, and are therefore not likely to be well-described under a typical semiconductor effective mass approximation; however, analysis of the effective masses should serve as a rough guide of the conduction properties. The calculated effective masses in the different lattice directions and high symmetry line from Γ to M are presented in Table 2. It is clear from the calculated masses that all conductivity takes place in the $[\text{Cu}_2\text{S}_2]^{2-}$ layers, and the material does not conduct in the c direction. The effective hole masses at the VBM are isotropic in both the a and b directions with effective masses of $2.8m_e$. The lowest hole masses occurs on the line from Γ to M and is $0.9m_e$.

It is instructive to note that a similar analysis of the industry standard n-type TCO, In_2O_3 , was carried out,

(79) Raebiger, H.; Lany, S.; Zunger, A. *Phys. Rev. B* **2007**, 76, 045209.

(80) Raebiger, H.; Lany, S.; Zunger, A. *Phys. Rev. Lett.* **2008**, 101, 027203.

(81) Nie, X. L.; Wei, S. H.; Zhang, S. B. *Phys. Rev. B* **2002**, 65, 075111.

(82) Kılıç, Ç.; Zunger, A. *Phys. Rev. Lett.* **2002**, 88, 095501.

(83) Segev, D.; Wei, S. H. *Phys. Rev. B* **2005**, 71, 125129.

and it resulted in an effective hole mass at the VBM of $16m_e$ and an effective electron mass at the CBM of $0.24m_e$.⁸⁴ If this is taken to be indicative of excellent n-type ability and very poor p-type ability, then the effective masses calculated for SCSOS suggest good p-type ability. This highlights that strong mixing of low binding energy cation states (here Cu 3d) with S 3p is required to provide valence band dispersion.

Discussion

It is becoming increasingly clear that Cu(I)-based TCOs based on the Delafossite or SrCu_2O_2 structure can never attain the level of conductivity needed to match the high performance n-type TCOs such as $\text{In}_2\text{O}_3:\text{Sn}$.⁸⁵ Delafossite materials will always be limited by their polaronic nature,^{71–74} which is actually unsurprising when you take into account the polaronic nature of the parent compound Cu_2O ,^{86–90} which displays typical resistivities of the order of $35 \Omega \text{ cm}$.⁹¹ Layered oxysulfides, however, have shown that they can be doped p-type with degenerate conduction,⁹² and thus offer perhaps the best opportunity for development of a high-quality p-type wide band gap material to rival their n-type counterparts.

Optimizing conductivity and transparency in layered oxychalcogenides is a very difficult task.²⁹ Replacement of S with Se or Te in the $[\text{Cu}_2\text{Ch}_2]^-$ layers can increase the p-type ability of these materials, but such an improvement normally comes at the expense of transparency.²⁹ A correlation between the basal lattice parameter (a) and band gap has been investigated for various layered oxychalcogenides and fluoride chalcogenides,²⁹ and the correlation is by no means linear. It is instructive to note that the bandgaps for Te based layered chalcogenides range between 2.2–2.4 eV regardless of lattice parameter while the Se based materials have bandgaps ranging from just under 3 eV (BaFCuSe , $a \approx 4.25 \text{ \AA}$) to $\sim 2.5 \text{ eV}$ (YCuOSe , $a \approx 3.9 \text{ \AA}$). The oxychalcogenides and fluoride chalcogenides that contain sulfur have band gaps between 3.2 eV and $\sim 3 \text{ eV}$, with the largest band gaps corresponding to basal lattice parameters bigger than 4.0 \AA , with SCSOS fitting nicely into that trend, having a basal lattice parameter of 4.08 \AA .³⁴

The reduction of the band gap when the basal lattice parameter is smaller, is ascribed to the shortening of the Cu–Cu distances in the $[\text{Cu}_2\text{Ch}_2]^-$ layers, which is

thought to result in the broadening of the valence band and conduction band.²⁹ This has been discussed in detail in the case of LaCuOSe (band gap of 2.8 eV) and YCuOSe (band gap of 2.3 eV).⁹³ In contrast to this, for Cu(I)-based Delafossite TCOs, the a lattice parameter does not control the band gap, but rather has an impact on the conductivity of these materials, as conductivity is known to occur via a polaronic, hopping mechanisms,^{71,73,74} with the Cu–Cu distances placing a limit on conductivity.

Interestingly, as SCSOS contains Sc as its trivalent cation in the perovskite like layer, doping with bigger trivalent cations like Y or La should increase the basal lattice parameter, increase the Cu–Cu distance, and possibly increase the transparency. Replacing Sr with Ba could also be another method of increasing the a lattice parameter. Undoubtedly, the ability to tune the transparency of SCSOS would be of much interest, but the ability to increase the p-type ability would be equally attractive. If the transparency could be increased by isovalent doping, to such an extent that doping with Se in the S site could be accommodated without decreasing the band gap below the 3.1 eV limit of transparency to visible light, then it is quite possible that an improved transparent conducting material could be designed.

Typically, hole carriers in layered oxychalcogenides are the product of Cu deficiency, and this could be the case for $[\text{Cu}_2\text{S}_2][\text{Sr}_3\text{Sc}_2\text{O}_5]$.³⁴ One of the advantages of the thick perovskite-like layer in SCSOS is that it provides a robust structural block, with two cation sites for p-type doping, and could be an extra source of cation deficiency, in both the Sr and Sc cation positions.³⁴ Defects and conductivity in layered oxychalcogenides have received limited experimental characterization, and surprisingly no theoretical attention. Undoped LaCuOSe has been reported to have a shallow acceptor level $\sim 20 \text{ meV}$ above the VBM with temperature dependent p-type conduction.⁹² Mg-doped LaCuOSe , however, exhibits no temperature dependence of hole concentration or mobility, indicating that it is a degenerate semiconductor,³³ with a conductivity as high as 910 S cm^{-1} . Thus it is quite plausible that doping of the Sc site with Ca or Mg would lead to a marked improvement in conductivity and possibly lead to degenerate semiconductor behavior, as has been demonstrated in the case of LaCuOSe:Mg .⁹² Alternatively doping of the Sr site with K, Na or Li would also increase the number of hole carriers in the material. Allied to the extremely high undoped conductivity reported for SCSOS, the exceptionally large mobility of holes in SCSOS indicate the possibility of much improved conductivity when doped p-type.³⁴ Thus SCSOS, which was originally synthesized as a candidate superconductor,⁷⁵ could possibly represent the ideal structural motif for designing high figure of merit p-type transparent conducting materials that are so sought after by materials

(84) Walsh, A.; Da Silva, J. L. F.; Wei, S. H. *Phys. Rev. B* **2008**, *78*, 075211.

(85) Mryasov, O. N.; Freeman, A. J. *Phys. Rev. B* **2001**, *64*, 233111.

(86) Hodby, J. W.; Jenkins, T. E.; Schwab, C.; Tamura, H.; Trivich, D. *J. Phys. C: Solid State Phys* **1976**, *9*, 1429–1439.

(87) Park, J. H.; Natesan, K. *Oxidation of Metals* **1993**, *39*, 411–435.

(88) Bose, A.; Basu, S.; Banerjee, S.; Chakravorty, D. *J. Appl. Phys.* **2005**, *98*, 074307.

(89) Scanlon, D. O.; Morgan, B. J.; Watson, G. W.; Walsh, A. *Phys. Rev. Lett.* **2009**, *103*, 096405.

(90) Scanlon, D. O.; Morgan, B. J.; Watson, G. W. *J. Chem. Phys.* **2009**, *131*, 124703.

(91) Madelung, O. M. *Semiconductors: Data Handbook*; Springer: Berlin, 2004.

(92) Hiramatsu, H.; Ueda, K.; Ohta, H.; Hirano, M.; Kamiya, T.; Hosono, H. *Thin Solid Films* **2003**, *445*, 304–308.

(93) Ueda, K.; Takafuji, K.; Yanagi, H.; Kamiya, T.; Hosono, H.; Hiramatsu, H.; Hirano, M.; Hamada, N. *J. Appl. Phys.* **2007**, *102*, 113714.

scientists. Further investigation of aliovalent and isovalent doping of SCSOS is thus warranted.

Conclusion

In this study, we have performed a detailed DFT examination of the new layered transparent conducting oxychalcogenide $[\text{Cu}_2\text{S}_2][\text{Sr}_3\text{Sc}_2\text{O}_5]$, using GGA corrected for on-site Coulombic interactions (GGA+ U) and a hybrid density functional (HSE06). $[\text{Cu}_2\text{S}_2]\text{-}[\text{Sr}_3\text{Sc}_2\text{O}_5]$ is found using HSE06 to possess a direct optical band gap of ~ 3.5 eV, which is a slight overestimation of the experimentally predicted optical band gap. Analysis of the band edges and effective masses indicate the potential for excellent p-type ability, consistent with

the experimentally reported high hole mobility. This increased hole mobility is caused by the favorable mixing of the S 3p states and the Cu 3d states at the valence band maximum.

Acknowledgment. This publication has emanated from research conducted with financial support of Science Foundation Ireland: PI Grant Number 06/IN.1/I92 and 06/IN.1/I92/EC07. We also acknowledge support from the HEA for the PTRLI programs IITAC (Cycle III) and e-INIS (CYCLE IV). All calculations were performed on the IITAC supercomputer as maintained by the Trinity Centre for High Performance Computing (TCHPC) and the Stokes computer, maintained by the Irish Centre for High-End Computing (ICHEC).